Iron−Sulfur Cluster Biosynthesis. Molecular Chaperone DnaK Promotes IscU-Bound [2Fe-2S] Cluster Stability and Inhibits Cluster Transfer Activity†

Shu-Pao Wu, Sheref S. Mansy, and J. A. Cowan*

Evans Laboratory of Chemistry, The Ohio State University, 100 West 18th Avenue, Columbus, Ohio 43210

Received August 7, 2004; Revised Manuscript Received December 9, 2004

ABSTRACT: IscU functions as a scaffold for Fe-S cluster assembly and transfer, and is known to be a substrate protein for molecular chaperones. Kinetic studies of Fe-S cluster transfer from holo IscU to apo Fd in the presence of chaperone DnaK demonstrate an inhibitory effect on the rate of Fe-S cluster transfer from IscU. Binding of DnaK reduces the rate of formation of the IscU−Fd complex (greater than 8-fold), but has little influence on the intrinsic rate of iron−sulfur cluster transfer to apo Fd. Apparently the molecular chaperone DnaK does not facilitate the process of Fe-S cluster transfer from IscU. Rather, DnaK has a modest influence on the stability of the IscU-bound Fe-S cluster that may reflect a more important role in promoting cluster assembly. In accord with prior observations the cochaperone DnaJ stimulates the ATPase activity of DnaK, but has a minimal influence on IscU cluster transfer activity, either alone or in concert with DnaK.

Heat shock proteins are molecular chaperones that bind unfolded, misfolded, and unstable polypeptides thereby preventing nonspecific aggregation processes (*1*, *2*). DnaK is a member of the highly conserved 70-kDa heat shock protein family (hsp70) and consists of two domains that have been crystallographically characterized as separate discrete species (*3*, *4*). The N-terminal domain of DnaK binds nucleotides (ATP and ADP), has ATPase activity, and interacts with the cochaperone DnaJ and the nucleotide exchange factor GrpE. The C-terminal domain consists of a conserved β-sandwich peptide-binding region with an α-helical lid. DnaK peptide substrates are rich in hydrophobic residues and thus bind to a hydrophobic pocket formed by the β-sandwich and the α-helical lid of the C-terminus of DnaK.

Recently, two molecular chaperones, Hsc66 and Hsc20, were identified in the *isc* (iron−sulfur cluster) operon (*5*). ISC proteins are integral components of iron−sulfur cluster biosynthesis pathways in a wide range of organisms, from Gram-positive and Gram-negative bacteria to archeae and eukaryotes, including humans. Of the ISC proteins, IscS and IscU appear to be the most critical. IscU assembles a nascent iron−sulfur cluster that is subsequently delivered to target proteins (*6*, *7*). IscS provides the sulfur equivalents to IscU for cluster biosynthesis. Other components include a [2Fe-2S] ferredoxin, alternate Fe-S scaffolds (IscA), and molecular chaperones Hsc66 and Hsc20. Although the roles of Hsc66 and Hsc20 in Fe-S cluster biosynthesis are not known, they have been shown to bind to IscU in vitro. Hsc66 is homologous to DnaK (41% identity for *E. coli*[1] proteins) and similarly possesses ATPase and peptide-binding domains. The ATPase activity of both proteins is stimulated by J-type cochaperones (DnaJ for DnaK and Hsc20 for Hsc66). Additionally, IscU and Hsc20 cooperatively stimulate the ATPase activity of *E. coli* Hsc66 (*8*). For eukaryotic systems, Ssq1 (Hsc66 homologue) and Jac1 (Hsc20 homologue) have been identified as mitochondrial components of the Fe-S cluster biosynthesis machinery (*9*). The hyperthermophile *Thermotoga maritima* lacks Hsc66 and Hsc20, but the genome does encode DnaK and DnaJ-homologues.

In this report, we demonstrate *Tm* DnaK binding to both *Tm* IscU and *Hs* ISU, and characterize the influence of this protein complex on cluster transfer activity and cluster stability. The role of the cochaperone DnaJ has also been explored and is shown to have minimal involvement in promoting cluster transfer activity. The remarkable similarity of the interaction of DnaK with *Tm* and *Hs* ISU-type proteins is of broader significance inasmuch as it demonstrates conserved structural and functional motifs in homologous families of proteins extending from bacteria and archeae through higher mammals. The data presented herein demonstrates an inhibitory influence of DnaK on cluster transfer to target proteins, as evidenced by the slower cluster transfer rates from IscU to a target apo Fd in the presence of DnaK, and introduction of sigmoidal behavior in the kinetic profile that is consistent with a consecutive-type reaction. Also, DnaK is observed to have a modest stabilizing influence on the IscU-bound Fe-S cluster that presumably reflects a role in facilitating formation of the IscU-bound cluster.

MATERIALS AND METHODS

General Chemicals. All solutions were argon-purged and handled under positive Ar(g) pressure using standard Schlenk

† This work was supported by a grant from the National Science Foundation, CHE-0111161 (J.A.C.).

* Author to whom correspondence should be addressed. Tel: 614 292 2703. Fax: 614 292 1685. E-mail: cowan@chemistry.ohio-state.edu.

[1] Abbreviations: ATP*, adenosine 5′-(β,γ-imido) triphosphate; BSA, bovine serum albumin; Cyt *c*, cytochrome *c*; DTT, dithiothreitol; *E. coli*, *Escherichia coli*; Fd, ferredoxin; FPLC, fast protein liquid chromatography; IPTG, isopropyl thiogalactoside; Hepes, 4-(2-hydroxyethyl)-1-piperazineethanesulfonic acid; *Hs*, *Homo sapiens*; isc, iron−sulfur cluster; LB medium, Luria-Bertani medium; NADPH, nicotinamide adenine dinucleotide phosphate; PAGE, polyacrylamide gel electrophoresis; PMSF, phenylmethylsulfonyl fluoride; PCR, polymerase chain reaction; SDS, sodium dodecyl sulfate; Tris, tris-(hydroxymethyl)-aminomethane; *Tm*, *Thermotoga maritima*; UV−vis, ultraviolet−visible.

10.1021/bi0483007 CCC: $30.25
Published on Web 02/19/2005

line techniques. Ni-NTA resin was purchased from QIAGEN (Valencia, CA). Both (CM-32 and DE-52) cation and anion exchange resins, respectively, were obtained from Whatman (Aston, PA). Sephadex G-75 and Superose-12 resins were from Pharmacia (Uppsala, Sweden). The reagents, NADPH, ATP, ATP* (adenosine 5′-(β,γ-imido) triphosphate), ADP and cytochrome *c* were all purchased from Sigma (St. Louis, MO). Hepes was purchased from Fisher (Fair Lawn, NJ), and Tris-HCl was purchased from Acros/Fisher (Fair Lawn, NJ).

Cloning of T. maritima DnaK and DnaJ. T. maritima genomic DNA was obtained from the American type culture collection (ATCC No. 43589D). Amplification of *dnaK* (TIGR locus: TM0373) was achieved by PCR using Pfu DNA polymerase and the following primers: 5′-GGGCCCGGCATATGGCAGAAAAGAAAGAATTCG-3′ and 5′-CCGGCCGGATCCTTACTGATTTGATGTTTCTCC-3′. The underlined regions denote *Nde*I and *Bam*HI sites, respectively. The thermocycle was identical to that described in the Stratagene manual. Digested PCR products were ligated with similarly treated vector (either pET21 or pET28). *E. coli* DH5α was transformed with the ligation mixture using the $CaCl_2$ method (*10*). Clones were confirmed by nucleotide sequencing at the Ohio State University Plant-Microbe Genomics Facility. Cloning into pET21 yielded a construct without a tag or additional residues (pTmDnaK). Cloning into pET28 resulted in the addition of an amino-terminal His-tag (pTmDnaKHis).

The cloning of *dnaJ* (TIGR locus TM0849) followed the same procedure as for *dnaK* except that the following primers were used: 5′-GGGCCCGGCATATGAAAAAAGAAAA-GAAGGAT-3′ and 5′- CCGGCCGGATCCTTAACCGATC-GTGACTCCGCG-3′, where the underlined regions denote *Nde*I and *Bam*HI sites, respectively. The gene was cloned into pET28 yielding a construct with an amino-terminal His-tag.

Protein Expression and Purification. E. coli BL21CodonPlus(DE3)-RIL was used for protein expression. A 100 mL Luria-Bertani culture (supplemented with either 50 μg/mL ampicillin and 35 μg/mL chloramphenicol for pTmDnaK constructs, or 50 μg/mL kanamycin and 35 μg/mL chloramphenicol for pTmDnaKHis constructs) was grown overnight as a starter culture. The culture was grown to an $A_{600} \sim 0.6$ prior to induction with 1 mM isopropyl-1-thio-β-D-galactopyranoside. Cells were pelleted 5 h after induction and stored at −80 °C for future use. The cell pellet was subsequently resuspended in 5 volumes of 50 mM Tris-HCl, pH 7.4, 1 mM EDTA, 1 mM β-mercaptoethanol, and 1 mM PMSF and sonicated. The lysate was incubated at 85 °C for 0.5 h, and the insoluble material was removed by centrifugation at 15000 rpm, 4 °C for 10 min. For the His-tagged construct, the cleared lysate was applied to a Ni-NTA column equilibrated with binding buffer (20 mM Tris-HCl, pH 7.9, 5 mM imidazole, 500 mM NaCl). The column was then washed with 5 column volumes of binding buffer, binding buffer + 5 mM imidazole, and then the protein was eluted with binding buffer + 195 mM imidazole. His-tagged protein was subsequently desalted by repeated ultrafiltration (Amicon) with 50 mM sodium phosphate, pH 7.4. For non-His-tagged constructs, streptomycin sulfate was added to 1% (w/v) and stirred at room temperature for 30 min. The sample was then centrifuged at 15000 rpm at 4 °C for 20 min and the supernatant loaded onto a G-75 gel filtration column equilibrated with 50 mM sodium phosphate, pH 7.4. Fractions were judged for purity by SDS−PAGE. All protein samples were stored at either 4 or −80 °C.

The conditions for cell growth in the case of DnaJ expression followed a similar protocol to that described for DnaK. Cell pellets were resuspended in 4 volumes (w/v) of 50 mM Tris-HCl, pH 7.4 and sonicated. Subsequently, the crude lysate was centrifuged at 15000 rpm, 4 °C for 0.5 h. The supernatant and pellet were purified separately. For the soluble fraction, the solution was added to a Ni-NTA column (Qiagen) equilibrated with binding buffer and washed with 5 column volumes of binding buffer followed by 5 column volumes of binding buffer + 10 mM imidazole. The protein was eluted with binding buffer + 200 mM imidazole. The insoluble cellular fraction was resuspended in 4 volumes (w/v) of 50 mM Tris-HCl, pH 7.9, 6 M urea. The solution was centrifuged at 15000 rpm, 4 °C for 0.5 h, and the pellet was discarded. The supernatant was loaded onto a Ni-NTA column equilibrated with binding buffer + 6 M urea. The column was washed with 5 column volumes of binding buffer + 6 M urea + 10 mM imidazole, and then the protein was eluted with binding buffer + 6 M urea + 300 mM imidazole. The protein solution was diluted 4-fold with 50 mM Tris-HCl, pH 7.9 and incubated at 4 °C with stirring overnight. The solution was centrifuged at 15000 rpm, 4 °C for 15 min, and the supernatant discarded. The pellet was resuspended in 100 mM Tris-HCl, 200 mM NaCl, 8 M Gdn-HCl, 1% tween-20, pH 7.4. β-Mercaptoethanol was added to 10 mM, and the solution was incubated at 70 °C for 10 min. The solution was allowed to slowly cool to room temperature, and then it was diluted 20-fold by the dropwise addition of 50 mM Tris-HCl, pH 7.4, 10 mM β-mercaptoethanol, 50 mM NaCl, 2 mM $ZnCl_2$ with stirring. A final centrifugation step was used to ensure the removal of any remaining insoluble material.

Expression and purification of human ISU (*Hs* ISU) and *T. maritima* IscU (*Tm* IscU) were performed as previously reported (*11*, *12*). Expression vectors for human ferredoxin (*Hs* Fd) and NADPH Fd reductase were kindly provided by J. L. Markley and G. Schulz, respectively, and purified as previously described (*13*, *14*).

UV−Vis Spectroscopy. UV−vis spectra were recorded on a Hewlett-Packard 8425A diode array spectrophotometer using the On-Line Instrument Systems (OLIS) 4300S operating system software. The concentrations of holo protein samples were determined from cluster extinction coefficients (*11*, *12*).

Iron Quantitation. Protein concentrations were quantitatively assessed from the measured extinction coefficient (above) and confirmed by calculations based on the Bio-Rad protein assay. Iron content was measured by the method of Moulis et al. (*15*). In brief, 200 μL of 0.05 mM protein was acidified by the addition of 60 μL of concentrated HCl. The sample was then heated to 100 °C for 15 min, and the precipitated material removed by centrifugation. The supernatant (100 μL) was diluted in 1.3 mL of 0.5 M Tris-HCl, pH 8.5. Subsequently, 0.1 mL of 5% freshly prepared sodium ascorbate and 0.4 mL of 0.1% bathophenanthrolinedisulfonate were added with mixing between each addition. After incubating at room temperature for 1 h, iron ion was quantitated from the measured absorbance at 535 nm and a previously constructed calibration curve made with 0.01 to 0.3 mM $FeCl_3$ solutions.

Cluster Degradation of Holo IscU. Holo *Tm* IscU was incubated in an HKM buffer (Hepes 50 mM, pH 7.5, KCl 150 mM, $MgCl_2$ 10 mM) with or without addition of DnaK (ADP) and DnaJ. The concentrations of *Tm* IscU, DnaK, DnaJ, ADP, and K_2HPO_4 were 50 μM, 200 μM, 200 μM, 2 mM, and 1 mM, respectively. Control experiments to determine the stabilizing influence of up to 15 mg/mL of BSA (Sigma) were also carried out. A 1.0 cm path-length cuvette was used for measurements. Cluster degradation was monitored at 412 nm, and the resulting absorbance versus time plots were fitted to a first-order exponential decay.

Calibration of Hs Fd Concentrations for Use in a Cytochrome c Assay (7). Under pre-steady-state conditions, the velocity of reduction of cytochrome *c* via a NADPH/Fd-reductase/Fd reduction pathway is related to the concentration of holo Fd. Reaction mixtures contained 80 μM cytochrome *c* and 200 nM Fd reductase in 1 mL of potassium phosphate buffer (10 mM, pH 7.5). Reactions were initiated by the addition of holo Fd and NADPH (400 μM) under anaerobic conditions and monitored by measuring the increase in absorbance at 550 nm from reduced cytochrome *c*. A 0.5 cm path-length cuvette was used for measurements, which were recorded anaerobically at room temperature. By varying the concentration of holo Fd (5−100 nM), calibration curves for reaction velocity (OD/30 s) versus concentration of Fd were constructed.

Determination of Reaction Rate Constants for [2Fe-2S] Cluster Transfer from Holo IscU to Apo Fd in the Presence of DnaK and DnaJ by the Cytochrome c Assay. Apo Fd (200 μM, 20 μL) was incubated with DTT (50 mM, 20 μL) for 10 min. Holo IscU was incubated with nucleotides (ADP and ATP) and various concentrations of DnaK and DnaJ in HKM buffer for 1 min. Subsequently, 10 μL of DTT reduced apo Fd was added to 50 μL of 200 μM holo *Hs* ISU or *Tm* IscU (previously incubated with DnaK for 1 min). At 10 min intervals, 6 μL of this mixture was withdrawn for evaluation of holo Fd formation by the cytochrome *c* assay. To eliminate the possibility of significant cluster transfer chemistry occurring during this transition phase, the sample was immediately diluted and assayed. The reaction mixture contained 80 μM cytochrome *c* and 200 nM Fd reductase in 1 mL of potassium phosphate buffer (10 mM, pH 7.5). The assay was initiated by the addition of 6 μL of holo IscU-apo Fd mixture and NADPH (400 μM) under anaerobic conditions. The final concentrations of Fd and IscU were 0.1 and 1 μM, respectively. The influence of BSA (up to 15 mg/mL) on cluster transfer kinetics was also examined. The reduction of Cty *c* was monitored by measuring the increase in absorbance at 550 nm. The pre-steady-state velocity (OD/30 s) was measured and used to determine the formation of reconstituted Fd according to the previously constructed calibration curves. The resulting plot of the yield of reconstituted Fd versus time was fitted by eq 1 (parameters defined in Figure 2), using Origin v.7 software from OriginLab corporation (Northampton, MA).

$$[\mathrm{Fd}] = a\{1-(k_2/(k_2-k_1)\exp(-k_1t))+(k_1/(k_2-k_1)\exp(-k_2t))\} \quad (1)$$

$$k_1 = [\mathrm{IscU}]_{\mathrm{total}}(k_{1a}+k_{1b}[\mathrm{DnaK}]/K_D)/(1+[\mathrm{DnaK}]/K_D) \quad (2)$$

$$k_2 = (k_{2a} + k_{2b}[\mathrm{DnaK}]/K_D)/(1 + [\mathrm{DnaK}]/K_D) \quad (3)$$

The obtained rate constants (k_1, k_2) were fitted to eqs 2 and 3 (Figure 5), and the rate constants (k_{1a}, k_{1b} k_{2a}, k_{2b}) and competitive dissociation constant (K_D) are listed in Table 2 (parameters defined in Figure 2). All reactions were examined at 25 °C, and data were determined at least in duplicate. As a control, the activity levels for apo Fd, apo IscU, and separate reactions that contained only one of the proteins, holo IscU or DnaK were analyzed, and all showed no activity. Furthermore, a correction was applied for the influence of DTT, which can reduce cytochrome *c* at a low rate compared to NADPH/Fd-reductase/Fd reduction, by measuring the rate of reduction of cytochrome *c* by DTT in a reaction mixture lacking NADPH and Fd reductase.

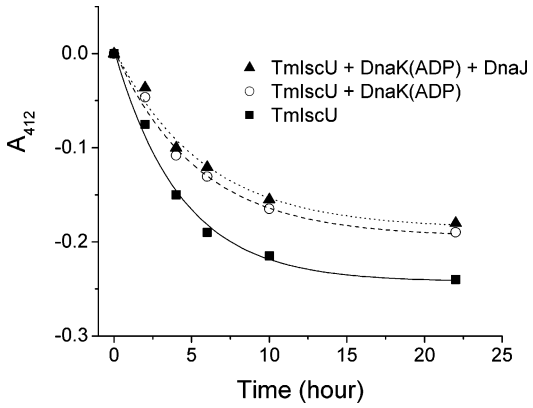

FIGURE 1: Cluster degradation of holo IscU. Holo *Tm* IscU was incubated in HKM buffer (Hepes 50 mM, pH 7.5, KCl 150 mM, $MgCl_2$ 10 mM) with or without addition of DnaK (ADP) and DnaJ. The concentrations of *Tm* IscU, DnaK, DnaJ, ADP, and K_2HPO_4 were 50 μM, 200 μM, 200 μM, 2 mM, and 1 mM. Cluster degradation was monitored at 412 nm and 25 °C, and the measured rate constants were 0.23 h^{-1}, 0.19 h^{-1} (DnaK-ADP), and 0.18 h^{-1} (DnaK-ADP + DnaJ).

RESULTS

Comparison with Prior Cloning, Purification, and Characterization of DnaK and DnaJ. Tm DnaK and *Tm* DnaJ were cloned from *T. maritima* chromosomal DNA both with (DnaK and DnaJ) and without an amino-terminal His-tag (DnaK). DnaK was previously cloned and characterized by Michelini and Flynn with a carboxy-terminal His-tag. (*16*). Our biochemical characterization of this protein yielded similar results with *Tm* DnaK displaying stability at high temperatures, a tendency to self-associate as evidenced by gel filtration profiles, and similar ATPase activity (0.02 min^{-1} at 25 °C). Additionally, we find no significant difference in activity between His-tagged and non-His-tagged proteins. *Tm* DnaJ expresses equally well, but is largely localized within the insoluble cellular fraction. Although we were able to isolate *Tm* DnaJ from the soluble fraction, the yield was too low for routine biochemical experiments. Therefore, we optimized conditions for the purification and refolding of *Tm* DnaJ isolated from the insoluble fraction. Consistent with prior observations on this class of chaperone (*8*, *17*, *18*), the cochaperone DnaJ was observed to stimulate the ATPase activity of DnaK up to 3-fold in the absence of IscU, and up to 17-fold if IscU was present.

Influence of DnaK and DnaJ on IscU-Bound Cluster Stability. IscU-bound Fe-S clusters are solvent-accessible and readily degraded (*7*, *19*). In the presence of DnaK, the stability of the bound [2Fe-2S] cluster is modestly enhanced and the rate constant for cluster degradation at physiological

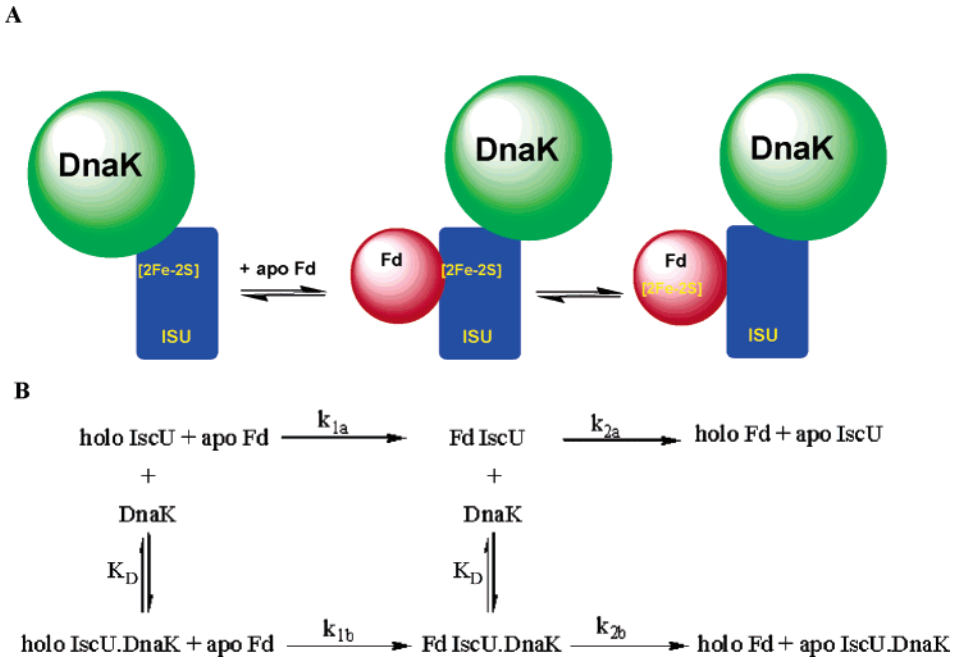

FIGURE 2: (A) Hypothetical model for the participation of DnaK in stabilization of the IscU-bound cluster and the competitive inhibitory influence on cluster transfer to a target apo Fd. (B) Reaction model for the rate laws defined by eqs 1−3.

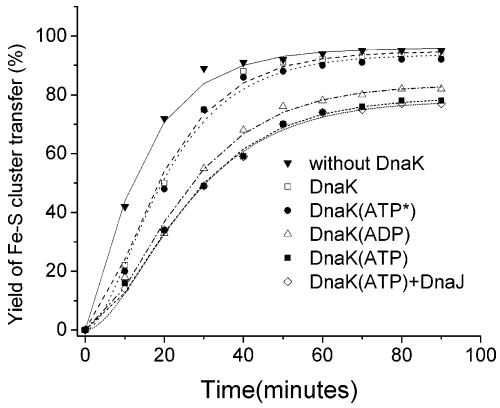

FIGURE 3: [2Fe-2S] cluster transfer from DnaK-bound holo *Tm* IscU to apo Fd (at 25 °C pH 7.4), in the presence of various nucleotides and DnaJ, was monitored by use of the cytochrome *c* assay (*7*). The concentrations of IscU, Fd, DnaK, and DnaJ were 167 μM, 16 μM, 420 μM, and 200 μM. The plot of the yield (%) of holo Fd as a function of reaction time was fitted by use of eq 1.

pH is decreased with measured rate constants of 0.23 h^{-1} in the absence of DnaK, 0.19 h^{-1} in the presence of DnaK-ADP, and 0.18 h^{-1} with both DnaK-ADP and DnaJ added (Figure 1). The presence of DnaJ has a minimal influence on cluster stability, possibly reflecting additional exclusion of solvent, but this effect was observed only in the presence of inorganic phosphate, consistent with the prior observation of ternary complex formation between DnaJ and a peptide·DnaK·ADP·phosphate complex (K_d = 0.14 μM) (*20*). As a further control the influence of up to 15 mg/mL of BSA on the stability of the IscU-bound cluster was examined under the conditions used; however, no significant effect was observed.

Cluster Transfer from Holo IscU to Apo Fd in the Presence of DnaK: Reaction Model. Transfer of a [2Fe-2S] cluster from holo IscU to apo Fd was monitored using a previously established cytochrome *c* assay (*7*). This assay is particularly valuable when *Hs* Fd is used as the reaction substrate since there is a high level of compatibility between *Hs* Fd and the NADPH-Fd reductase used to mediate electron-transfer between holo Fd and cytochrome *c*. We have previously observed that *Tm* IscU is able to mediate [2Fe-2S] cluster transfer to apo *Hs* Fd (*12*). In fact, we have measured relative rate constants of 0.073 min^{-1} and 0.086 min^{-1} for *Tm* IscU and *Hs* ISU [2Fe-2S] transfer, respectively, to apo *Hs* Fd. As demonstrated below, the apparent structural and functional similarity between bacterial and human homologues also extends to the influence of *Tm* chaperone DnaK.

To maintain pseudo-first-order conditions the concentration of IscU was at least 10-fold higher than that of Fd. To observe the effect of DnaK on cluster transfer, reactions were carried out in the presence and absence of DnaK. Significantly, the binding of DnaK to IscU does not completely inhibit the reaction, even at saturating concentrations of DnaK, but rather the molecular chaperone decreases the rate constant by a factor of 2. Also, a pronounced lag phase was observed with increasing concentration of DnaK. Interestingly, a direct relationship between the concentration of DnaK and the length of the initial lag phase of the reaction was observed. To account for this reaction profile in the kinetics of cluster transfer, a two-step consecutive reaction model was proposed that includes formation of an IscU−Fd complex (k_1) followed by cluster transfer (k_2) (eq 1 and Figure 2), where K_D is the competitive dissociation constant for the holo IscU/DnaK complex in the presence of ferredoxin. Figures 3 and 4 show a fit of eq 1 to the time-dependence of Fe-S cluster transfer from *Tm* IscU or *Hs* ISU to apo Fd. The dependence of k_1 and k_2 on DnaK concentration was further evaluated by use of eqs 2 and 3 (Figure 5). The constants k_{1a} and k_{1b} correspond to the rates of formation of Fd·IscU and Fd·IscU·DnaK complexes, respectively. Rate constants k_{2a} and k_{2b} correspond to Fe-S cluster transfer within the complexes, Fd·IscU and Fd·IscU·DnaK, respectively. These parameters were determined from the dependence of the observed reaction rate constants on the concentration of DnaK, and these activities were determined

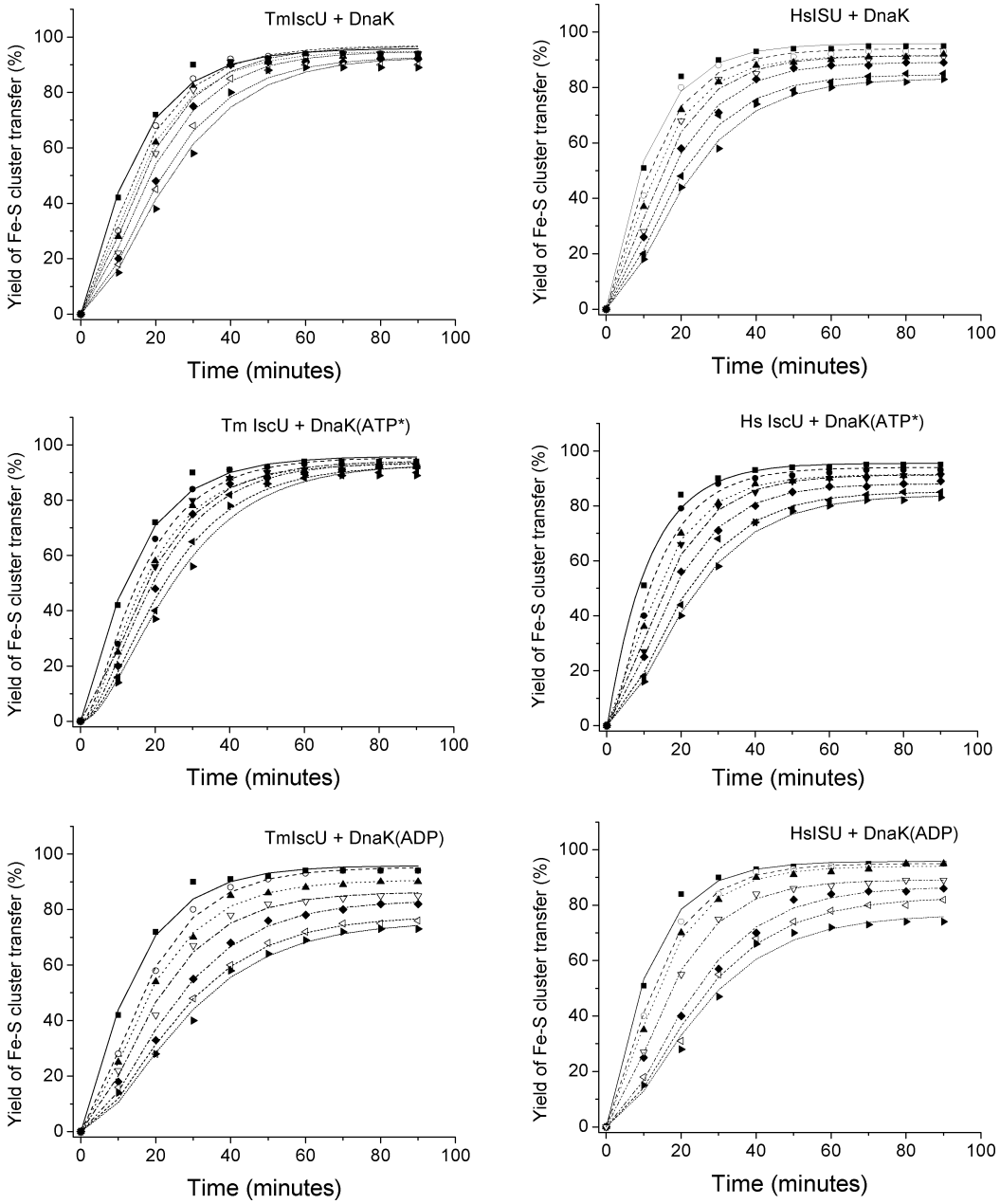

FIGURE 4: Transfer of the IscU(ISU)-bound [2Fe-2S] cluster to apo Fd (at 25 °C) was monitored by use of the cytochrome *c* assay (*7*). Each symbol represents a different concentration of DnaK (50, 105, 210, 420, 630, 780 μM). The overall concentrations of apo Fd and IscU were 16 and 167 μM, respectively. Plots of the yield (%) of holo Fd as a function of reaction time were fitted by use of eq 1.

in the presence and absence of bound nucleotides (ADP, ATP, and the nonhydrolyzable ATP analogue adenosine 5′-(β,γ-imido) triphosphate, designated ATP*). Analogous experiments were also carried out in the presence of the cochaperone DnaJ, although as detailed below these provided similar results (Figure 3), and so DnaJ appears to serve no significant role for cluster transfer reactions and is not explicitly shown in Figure 2.

Cluster Transfer from Holo IscU to Apo Fd in the Presence of DnaK and DnaJ: Reaction Profiles. The reaction scheme illustrated in Figure 2 necessarily implies the appearance of a lag phase, since sigmoidal behavior is commonly observed for a two-step consecutive reaction in the limit where $k_1 \sim k_2$. The likelihood that the proposed reaction model is valid is substantiated both by the excellent fits obtained to the experimental data, and by the reasonableness of the fitted parameters for the reaction chemistry that is described.

Figure 3 shows the process of Fe-S cluster transfer from DnaK-bound *Tm* IscU to apo Fd in the presence of various nucleotides and DnaJ. DnaK binding to IscU influences the process of Fe-S cluster transfer from holo IscU to apo Fd, especially the formation of the complex IscU−Fd. Nucleotide-free DnaK shows a higher value for the ratio k_1/[IscU], relative to nucleotide-bound DnaK's. As is evident from eq 2, the ratio k_1/[IscU] reflects the association constant for IscU binding to apo Fd, where IscU may be free or bound by DnaK. This association rate is observed to be higher in the absence of bound nucleotide (Table 1). The rate for the nonhydrolyzable ATP*-bound form of DnaK lies between the nucleotide-free form and nucleotide-bound forms of DnaK. The similarity of results for ATP- versus ADP-bound forms of DnaK is not unexpected inasmuch as the ATP-bound form will be converted to the ADP-bound state. The only significant difference occurs in the early stages of the

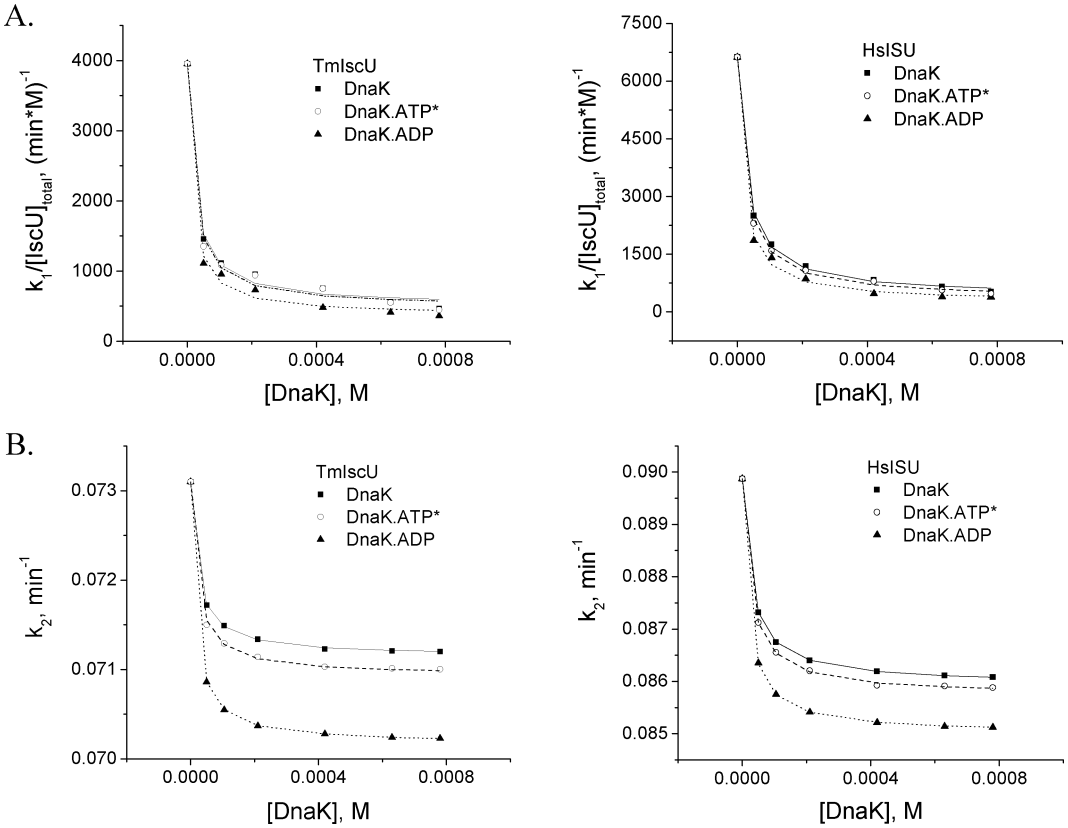

FIGURE 5: (A) Plots of k_1 versus concentration of DnaK. (B) Plots of k_2 versus concentration of DnaK.

Table 1: Observed Rate Constants for IscU Binding to Apo Fd, and [2Fe-2S] Cluster Transfer from DnaK-Bound Holo IscU to Apo Fd in the Presence of Various Nucleotides and DnaJ[a]

complexes	k_1/[IscU], $(M\ min)^{-1}$	k_2, $(min)^{-1}$
Tm IscU/DnaK	755 ± 40	0.071 ± 0.002
Tm IscU/DnaK-ATP*	550 ± 25	0.071 ± 0.002
Tm IscU/DnaK-ADP	481 ± 23	0.070 ± 0.002
Tm IscU/DnaK-ATP	450 ± 20	0.070 ± 0.002
Tm IscU/DnaK-ATP/DnaJ	440 ± 20	0.070 ± 0.002

[a] These experiments were carried out at a fixed concentration of IscU and DnaK. The concentrations of IscU, Fd, DnaK, and DnaJ were 167 μM, 16 μM, 420 μM, and 200 μM. The concentrations of ATP, ATP*, and ADP were 3.3 mM.

Table 2: Rate Constants for Fe-S Cluster Transfer from Holo IscU (ISU) to Apo Fd[a]

complexes	k_{1b} $(M\ min)^{-}1$	k_{2b} (min^{-1})	K_D (μM)
Tm IscU/DnaK/Hs Fd	506 ± 24	0.071 ± 0.002	21 ± 2
Tm IscU/DnaK-ATP*/Hs Fd	491 ± 22	0.071 ± 0.002	20 ± 2
Tm IscU/DnaK-ADP/Hs Fd	373 ± 20	0.070 ± 0.002	15 ± 1
Hs ISU/DnaK/Hs Fd	416 ± 20	0.086 ± 0.002	27 ± 2
Hs ISU/DnaK-ATP*/Hs Fd	348 ± 15	0.086 ± 0.002	25 ± 2
Hs ISU/DnaK-ADP/Hs Fd	239 ± 10	0.085 ± 0.002	19 ± 1

[a] Rate constants k_{1a} and k_{2a} for *Tm* IscU/*Hs* Fd are 3954 ± 210 M^{-1} min^{-1} and 0.073 ± 0.001 min^{-1}, respectively. Rate constants k_{1a} and k_{2a} for *Hs* ISU/*Hs* Fd are 6624 ± 320 M^{-1} min^{-1} and 0.086 ± 0.002 min^{-1}, respectively.

cluster transfer reaction promoted by DnaK-ATP (Figure 3), when the initial yield of cluster transfer in the presence of DnaJ is slightly lower than that observed in its absence. Again, addition of BSA had no significant influence on the cluster transfer profile.

From the dependence of k_1 on DnaK concentration the magnitudes of k_{1a} and k_{1b} were determined (Figure 5). Table 2 illustrates how the values of k_{1b} are smaller than those observed for k_{1a}. For example, k_{1a} is ~3954 M^{-1} $min-1$ for *Tm* IscU, whereas that for *Tm* ISU/DnaK, *Tm* ISU/DnaK-ATP*, and *Tm* ISU/DnaK-ADP is 506 M^{-1} min^{-1}, 491 M^{-1} min^{-1}, and 373 M^{-1} min^{-1}, respectively. The value of k_{1a} is found to be 8- to 11-fold higher than that determined for k_{1b}. Similarly, k_{1a} is ~ 6624 M^{-1} min^{-1} for *Hs* ISU, whereas that for *Hs* ISU/DnaK, *Hs* ISU/DnaK-ATP*, and *Hs* ISU/DnaK-ADP is 416 M^{-1} min^{-1}, 348 M^{-1} min^{-1}, and 239 M^{-1} min^{-1}, respectively. For *Hs* ISU, the k_{1a} (*Hs* ISU) is 15- to 27-fold greater than that of k_{1b}. The relatively low values of k_{1b} indicate that DnaK binding to IscU influences formation of the holo IscU/apo Fd complex. Comparison of the k_{1a} values shows that *Hs* ISU more rapidly binds to *Hs* Fd than the reaction between *Tm* IscU and *Hs* Fd. This is consistent with facilitated intraspecies protein interactions.

Although the values of k_{2a} are slightly higher than k_{2b}, the differences are minor. For example, the k_{2a} of *Tm* IscU is 0.073 min^{-1}, whereas that for *Tm* IscU/DnaK, *Tm* IscU/DnaK-ATP*, and *Tm* IscU/DnaK-ADP is 0.071 min^{-1}, 0.071 min^{-1}, and 0.070 min^{-1}, respectively. Similar trends are observed for *Hs* ISU. The small differences between k_{2a} and k_{2b} indicate that DnaK binding to IscU does not greatly influence Fe-S cluster transfer between IscU and Fd. Although the binding of DnaK to IscU inhibits the formation of the Fd/IscU complex, it does not influence the Fe-S cluster reaction.

The apparent dissociation constant, K_D, for the complex of DnaK and IscU lies in the range 15−27 μM (Table 2), which is reasonable for the binding of a hydrophobic peptide to DnaK (*21*), especially in the presence of a competing

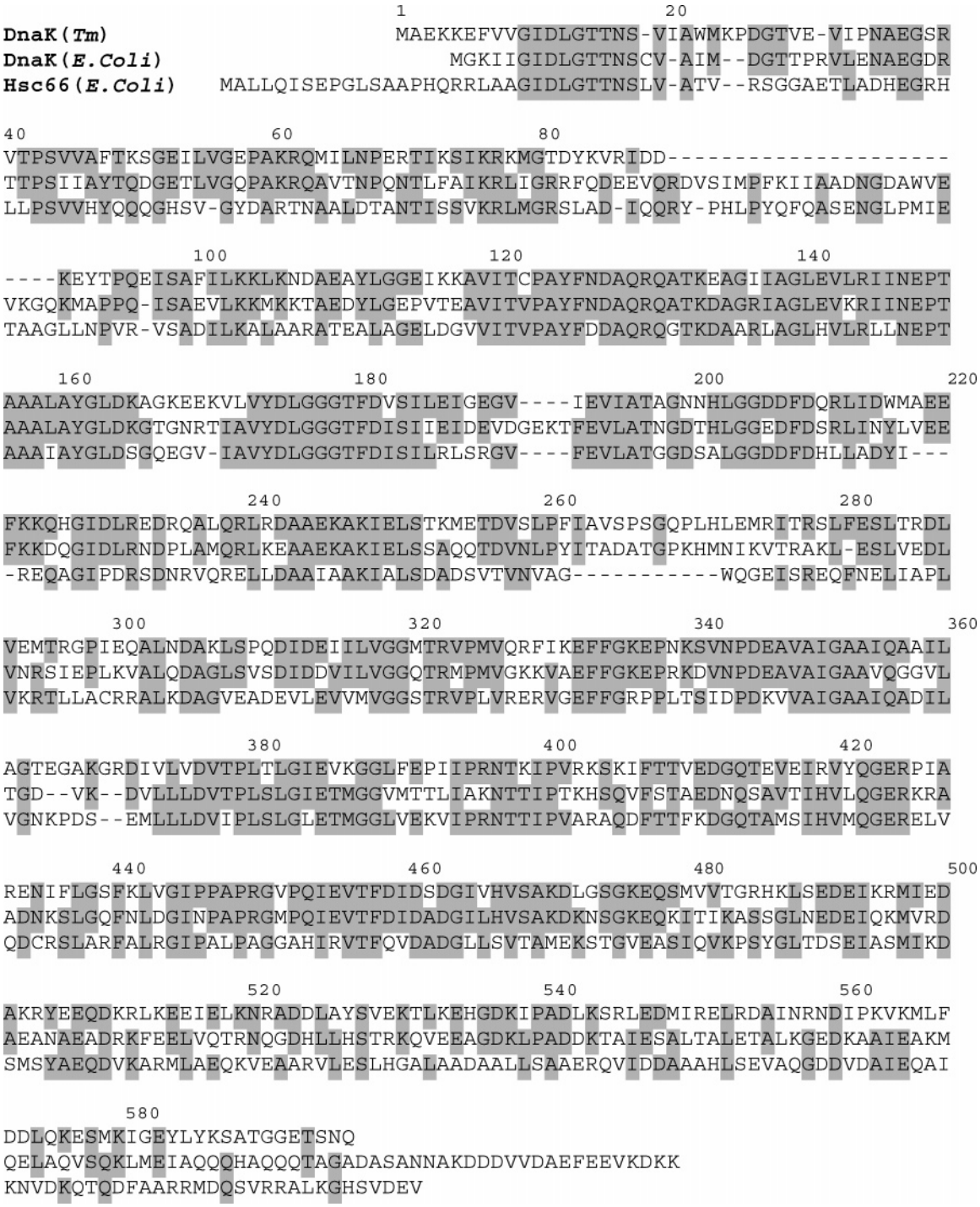

FIGURE 6: Sequence alignment of *Tm* DnaK, *E. coli* DnaK, and *E. coli* Hsc66. Identical residues are shaded.

ferredoxin protein. DnaK appears to possess a lower K_D for IscU in the presence of nucleotides (ATP and ADP). Dissociation constants were not determined in the presence of the DnaJ since the kinetic results on which the measurement is based proved similar in the presence and absence of the cochaperone.

DISCUSSION

T. maritima DnaK is a 596 residue protein with a molecular weight of 66 kDa (*16*). It contains two domains: an ATPase domain (1−362), and a peptide binding domain that consists of a β-sandwich (363−489) and an α-helical lid (490−596). In Figure 6, the sequence of *Tm* DnaK is seen to be homologous to that of the DnaK and Hsc66 proteins from *E. coli*, with the exception of a 25-amino acid deletion following residue 89. *Tm* DnaK has 53% sequence identity with *E. coli* DnaK and 40% with *E. coli* Hsc66, while *E. coli* DnaK has 41% sequence identity with *E. coli* Hsc66. The overall sequence homology of the three proteins is 31%. Comparison of each domain of the three proteins shows that the percent homologies are 35% (ATPase domain), 38% (β-sandwich), and 9% (C-terminal α-helical lid). Clearly DnaK and Hsc66 are highly homologous over the ATPase and peptide-binding domains. As is commonly observed (*22*), the sequence homology is significantly lower in the α-helical lid.

Previous work has demonstrated *E. coli* IscU to complex with two molecular chaperones, namely, Hsc66 (HscA) and Hsc20 (HscB) (*8*, *23*). Hsc66 binds to residues 99−103 (LPPVK) of IscU, and the binding of IscU stimulates the ATPase activity of Hsc66. Hsc20 also binds to IscU and facilitates the interaction of IscU with Hsc66. On the basis of these binding observations, it has been suggested that the molecular chaperones might facilitate iron−sulfur cluster transfer (*8*). However, no experimental evidence has been reported to support the proposed functions of molecular chaperones in this process. DnaK is generally associated with cellular housekeeping roles, such as preventing protein aggregation and denaturation. Since it is specifically located in the *isc* operon, Hsc66 has been assigned a more specific cellular role, especially in iron−sulfur cluster biosynthesis (*8*). However, *T. maritima* lacks an Hsc66 homologue, and so it is reasonable to expect that DnaK is acting in the capacity of Hsc66. In fact DnaK has broader specificity than Hsc66, but has been shown to bind to the same region of IscU as Hsc66, consistent with a similar role in cellular cluster assembly. The results described here demonstrate that DnaK can bind to IscU and influences both the stability of IscU-bound Fe-S clusters and the rate of iron−sulfur cluster transfer to a target protein, but in an unexpected fashion.

Comparison of Tm IscU versus Hs ISU Cluster Transfer Activity toward a Hs Fd Target. Tm is an evolutionarily ancient organism (*24*); nevertheless, the *Tm* IscU protein shows relatively high homology (26% identity and 30% without the insert) to its human counterpart (*12*). Both *Tm* IscU and *Hs* ISU show relatively high activity in cluster transfer to an apo *Hs* Fd target (0.073 min^{-1} and 0.086 min^{-1} for *Tm* IscU versus *Hs* ISU, respectively). Moreover, *Tm* DnaK displays similar influences on the reaction of both *Tm* IscU and *Hs* ISU, with cluster transfer to *Hs* Fd displaying a significant lag phase in each cluster transfer reaction (Figure 4). These results clearly demonstrate the important roles of molecular chaperones in iron−sulfur cluster biosynthesis, but also speak to conserved structural and functional motifs in homologous families of proteins extending from bacteria and archeae through higher mammals. These data also provide a strong justification for the cross use of *Tm* and *Hs* proteins for functional and mechanistic studies.

The Influence of DnaK and DnaJ on IscU-Bound Cluster and Stability. We have previously shown that IscU-bound [2Fe-2S] clusters are prone to hydrolytic degradation (*7*). The relative rate of cluster hydrolysis ultimately depends on both the relative binding energies of the Fe-S center to protein ligands and the solvent accessibility of the clusters. The influence of chaperones on the kinetics of cluster hydrolysis was examined at physiological pH, and the experimental data clearly demonstrates DnaK binding to holo IscU to slow the rate of cluster loss (Figure 1). All stability experiments were repeated in the presence of DnaJ, and the results were found to be similar to those obtained with DnaK alone. Accordingly, under conditions of saturating DnaK, DnaJ serves no significant role in promoting the stability of the IscU-bound cluster.

Inasmuch as complex formation between DnaK and IscU is unlikely to change the bond energies for ligation of the Fe-S cluster to IscU, the observed protection most likely reflects a change in solvent accessibility following chaperone binding. While the influence on stability is modest, it is also likely that this is a manifestation of a more direct role of chaperones in mediating the assembly of the IscU-bound cluster, which requires deliver of both iron ion and sulfide coordination (*25*). In this regard, NMR solution structural studies of *Tm* IscU (*26*) and other biophysical measurements (*27*) have previously demonstrated unusual dynamic behavior for this protein family. The secondary structure of *Tm* IscU is well defined, with six α-helixes and three β-strands; howeve, its tertiary structure appears to be fluxional among distinct conformational states (*27*). DnaK may bind, and protect from solvent, a specific conformation for the iron-bound intermediate, conferring sufficient stability to allow final formation of the IscU-bound [2Fe-2S] center.

Cluster Transfer from Holo IscU to Apo Fd in the Presence of DnaK and DnaJ. Previously, it has been shown that the *E. coli* chaperones Hsc66 and DnaK both bind to IscU (*8*); however, the functional consequence of molecular chaperone binding had not been described. Here we demonstrate that in the presence of DnaK the Fe-S cluster transfer reaction from holo IscU to apo Fd is dramatically influenced. Figure 2 shows a two-step consecutive reaction model that is consistent with the observed rate data: namely, formation of the Fd·IscU complex (k_1) followed by cluster transfer (k_2). DnaK putatively binds to IscU through a conserved motif (*23*), but rather than promoting cluster transfer it appears to slow down the reaction and lower the yield of Fe-S cluster transfer (Figures 3 and 4). When k_1 is comparable in value to k_2, a lag phase is both expected and observed. The experimental data clearly demonstrate an inhibitory influence by DnaK on cluster transfer, with the transfer rate observed to decrease by a factor of 2. We have attempted to explain the role of the *Tm* homologues in mediating IscU cluster transfer in terms of a detailed reaction model (Figure 2) that demonstrates an outstanding fit of experimental data to the derived rate law. Inasmuch as the inhibitory influence of DnaK is not complete, it is suggested that DnaK remains bound to IscU during the cluster transfer reaction.

The experimental data clearly indicates that the rate of formation of the IscU/Fd complex is decreased in the presence of DnaK. More specifically, the rate constants k_1 (complex formation) and k_2 (Fe-S cluster transfer) are both decreased in the presence of DnaK. Since the rate of formation of IscU/Fd (k_{1a}) is significantly greater than the formation of a tertiary complex (Fd/IscU/DnaK, k_{1b}) (8- to 11-fold for *Tm* IscU and 15- to 27-fold for *Hs* ISU), DnaK binding to IscU must inhibit complex formation between IscU and Fd. By comparison, the difference between the rate constants of Fd/IscU (k_{2a}) and Fd/IscU/DnaK (k_{2b}) cluster transfer is relatively small. Therefore, DnaK does not directly promote cluster transfer chemistry, but rather interferes with complex formation of the target protein (in this case apo Fd) with IscU. The inhibitory influence of apo Fd on DnaK binding is also manifest by the increase in the apparent dissociation constant, K_D, for the complex of DnaK and IscU (15−27 μM, Table 2), relative to direct binding of chaperone to IscU (∼1.6 μM for *E. coli* Hsc66 binding to IscU) (*28*) and binding of a hydrophobic peptide to DnaK (K_D = 0.06 to 2 μM) (*21*).

Cluster transfer reactivity was also examined in the presence of DnaJ (Figure 3), and the results were found to be similar to those obtained with DnaK alone. Accordingly, under conditions of saturating DnaK, DnaJ serves no

significant role in promoting cluster transfer to a target protein.

Comparison of Tm IscU and Hs ISU Interaction with DnaK. E. coli Hsc66 and DnaK bind to a conserved motif on IscU near a conserved Fe-S ligating Cys (Cys 124) (*23*). There are several possible influences of this binding event on target protein interactions. First, the binding of DnaK may change the surface charge distribution on IscU. Since protein−protein interactions are often dependent on surface charge distribution, a perturbation of this charge distribution by DnaK binding may alter the affinity of target proteins for IscU. Second, binding of DnaK to IscU may simply sterically hinder Fd binding to IscU. X-ray diffraction structures show that peptide substrates bind to the β-sandwich/helical lid domains of DnaK. Since DnaK (66 kDa) is significantly larger than IscU (16 kDa) and Fd (13 kDa), binding of DnaK to IscU may block Fd binding.

Previously it has been shown that *E. coli* Hsc66 binds to *E. coli* IscU with micromolar affinity (*28*). The consensus motif within IscU that is recognized by the chaperone Hsc66 is hydrophobic-Pro-Pro-hydrophobic-hydrophilic, in which the final hydrophilic is a basic residue. In *E. coli* and most higher organisms this motif is LPPVK. However, in more lowly evolved bacteria, including *T. maritima*, this motif is not strictly conserved and often has a hydrophilic residue in place of the first hydrophobic and an aromatic substituted for the first proline. In *T. maritima* it spans residues 117−121 and is NYPAR. Interestingly, it appears that IscU homologues with this altered chaperone binding motif also possess a structured ~18 amino acid insert between α3 and α4 (*12*). Furthermore, organisms encoding such IscU homologues often do not code for Hsc66. However, these organisms do code for DnaK, a chaperone that has the ability to bind to the same motif on IscU as Hsc66 (*23*). The implications of such differences in IscU proteins from different organisms are not readily apparent, particularly since their cluster transfer activities are similar.

Relevance of DnaK ATPase Activity in Cluster Transfer. The N-terminal domain of DnaK binds nucleotides (ATP and ADP), has ATPase activity, and interacts with cochaperone DnaJ and the nucleotide exchange factor GrpE (*29*, *30*). The C-terminal domain consists of a conserved β-sandwich peptide-binding region with an α-helical lid. DnaK peptide substrates are rich in hydrophobic residues and thus bind to a hydrophobic pocket formed by the β-sandwich and the α-helical lid of the C-terminus of DnaK. The reaction cycle is typically fueled by the binding and hydrolysis of ATP and is regulated by cochaperones DnaJ and GrpE (*29*, *30*). More specifically, DnaK alternates between an ATP-bound form, which has a low peptide affinity, and an ADP-bound form, which has a relatively high substrate affinity. DnaJ typically promotes substrate binding to the ATP-bound state and stimulates ATP hydrolysis, where the nucleotide exchange factor GrpE promotes ADP dissociation. Substrate release occurs in concert with ATP binding. It is believed that the DnaK/DnaJ/GrpE reaction cycle and the energy derived from ATP hydrolysis produces a conformational change in the protein substrate that increases the probability of proper folding (*20*, *21*, *30*, *31*).

These observations notwithstanding, it is clear from the data shown in Tables 1 and 2, and Figures 3, 4, and 5, that the ATPase activity of DnaK, and the nucleotide-bound state has very little influence on the intrinsic cluster transfer activity, impacting only the binding affinity for IscU. This is entirely consistent with the wealth of literature that supports a role for nucleotide in defining the kinetic and thermodynamic parameters for DnaK binding to cognate peptides (*20*, *21*, *30*, *31*), with the cochaperone DnaJ and nucleotide exchange factor GrpE regulating these parameters.

REFERENCES

1. Bukau, B., and Horwich, A. L. (1998) The Hsp70 and Hsp60 chaperone machines, *Cell 92*, 351−366.
2. Harlt, F. U. (1996) Molecular chaperones in cellular protein folding, *Nature 381*, 571−579.
3. Zhu, X., Zhao, X., Burkholder, W. F., Gragerov, A., Ogata, C. M., Gottesman, M. E., and Hendrickson, W. A. (1996) Structural analysis of substrate binding by the molecular chaperone DnaK, *Science 272*, 1606−1614.
4. Harrison, C. J., Hayer-Hartl, M., Di Liberto, M., Hartl, F., and Kuriyan, J. (1997) Crystal structure of the nucleotide exchange factor GrpE bound to the ATPase domain of the molecular chaperone DnaK, *Science 276*, 431−435.
5. Zheng, L., Cash, V. L., Flint, D. H., and Dean, D. R. (1998) Assembly of iron-sulfur clusters. Identification of an iscSUA-hscBA-fdx gene cluster from Azotobacter vinelandii, *J. Biol. Chem. 273*, 13264−13272.
6. Agar, J. N., Zheng, L., Cash, V. L., Dean, D. R., and Johnson, M. K. (2000) Role of the IscU Protein in Iron-Sulfur Cluster Biosynthesis: IscS-mediated Assembly of a $[Fe_2S_2]$ Cluster in IscU, *J. Am. Chem. Soc. 122*, 2136−2137.
7. Wu, S., Wu, G., Surerus, K. K., and Cowan, J. A. (2002) Iron-Sulfur Cluster Biosynthesis. Kinetic Analysis of [2Fe-2S] Cluster Transfer from Holo ISU to Apo Fd: Role of Redox Chemistry and a Conserved Aspartate, *Biochemistry 41*, 8876−8885.
8. Hoff, K. G., Silberg, J. J., and Vickery, L. E. (2000) Interaction of the iron-sulfur cluster assembly protein IscU with the Hsc66/Hsc20 molecular chaperone system of Escherichia coli, *Proc. Natl. Acad. Sci. U.S.A. 97*, 7790−7795.
9. Lutz, T., Westermann, B., Neupert, W., and Herrmann, J. M. (2001) The mitochondrial proteins Ssq1 and Jac1 are required for the assembly of iron sulfur clusters in mitochondria, *J. Mol. Biol. 307*, 815−825.
10. Sambrook, J., Fritsch, E. F., and Maniatis, T. (1989) Molecular Cloning, *Cold Spring Harbor Laboratory Press*.
11. Foster, M. W., Mansy, S. S., Hwang, J., Penner-Hahn, J. E., Surerus, K. K., and Cowan, J. A. (2000) A Mutant Human IscU Protein Contains a Stable $[2Fe\text{-}2S]^{2+}$ Center of Possible Functional Significance, *J. Am. Chem. Soc. 122*, 6805−6806.
12. Mansy, S. S., Wu, G., Surerus, K. K., and Cowan, J. A. (2002) Iron-sulfur cluster biosynthesis. Thermatoga maritima IscU is a structured iron-sulfur cluster assembly protein, *J. Biol. Chem. 277*, 21397−21404.
13. Xia, B., Cheng, H., Bandarian, V., Reed, G. H., and Markley, J. L. (1996) Human Ferredoxin: Overproduction in Escherichia coli, Reconstitution in Vitro, and Spectroscopic Studies of Iron−Sulfur Cluster Ligand Cysteine-to-Serine Mutants, *Biochemistry 35*, 9488−9495.
14. Ziegler, G. A., Vonrhein, C., Hanukoglu, I., and Schulz, G. E. (1999) The structure of adrenodoxin reductase of mitochondrial P450 systems: electron transfer for steroid biosynthesis, *J. Mol. Biol. 289*, 981−990.
15. Moulis, J. M., and Meyer, J. (1982) Characterization of the selenium-substituted 2 [4Fe-4Se] ferredoxin from Clostridium pasteurianum, *Biochemistry 21*, 4762−4771.
16. Michelini, E. T., and Flynn, G. C. (1999) The unique chaperone operon of Thermotoga maritima: cloning and initial characterization of a functional Hsp70 and small heat shock protein, *J. Bacteriol. 181*, 4237−4244.
17. Silberg, J. J., and Vickery, L. E. (2000) Kinetic characterization of the ATPase cycle of the molecular chaperone Hsc66 from Escherichia coli, *J. Biol. Chem. 275*, 7779−7786.
18. Silberg, J. J., Hoff, K. G., and Vickery, L. E. (1998) The Hsc66-Hsc20 chaperone system in Escherichia coli: chaperone activity and interactions with the DnaK-DnaJ-grpE system, *J. Bacteriol. 180*, 6617−6624.
19. Wu, G., Mansy, S. S., Wu, S., Surerus, K. K., Foster, M. W., and Cowan, J. A. (2002) Characterization of an Iron−Sulfur Cluster

Assembly Protein (ISU1) from Schizosaccharomyces pombe, *Biochemistry 41*, 5024−5032.
20. Pierpaoli, E. V., Sandmeier, E., Schonfeld, H.-J., and Christen, P. (1998) Control of the DnaK chaperone cycle by substoichiometric concentrations of the co-chaperones DnaJ and GrpE, *J. Biol. Chem. 273*, 6643−6649.
21. Pierpaoli, E. V., Gisler, S. M., and Christen, P. (1998) Sequence-Specific Rates of Interaction of Target Peptides with the Molecular Chaperones DnaK and DnaJ, *Biochemistry 37*, 16741−16748.
22. Chou, C., Forouhar, F., Yeh, Y., Shr, H., Wang, C., and Hsiao, C. (2003) Crystal Structure of the C-terminal 10-kDa Subdomain of Hsc70, *J. Biol. Chem. 278*, 30311−30316.
23. Hoff, K. G., Ta, D. T., Tapley, T. L., Silberg, J. J., and Vickery, L. E. (2002) Hsc66 Substrate Specificity Is Directed toward a Discrete Region of the Iron-Sulfur Cluster Template Protein IscU, *J. Biol. Chem. 277*, 27353−27359.
24. Bocchetta, M., Gribaldo, S., Sanangelantoni, A., and Cammarano, P. (2000) Phylogenetic Depth of the Bacterial Genera Aquifex and Thermatoga Inferred from Analysis of Ribosomal Protein, Elongation Factor, and RNA Polymerase Subunit Sequences, *J. Mol. Evol. 50*, 366−380.
25. Nuth, M., Yoon, T., and Cowan, J. A. (2002) Iron-Sulfur Cluster Biosynthesis: Characterization of Iron Nucleation Sites for Assembly of the $[2Fe\text{-}2S]^{2+}$ Cluster Core in IscU Proteins, *J. Am. Chem. Soc. 124*, 8774−8775.
26. Bertini, I., Cowan, J. A., Del Bianco, C., Luchinat, C., and Mansy, S. S. (2003) Thermotoga maritima IscU. Structural Characterization and Dynamics of a New Class of Metallochaperone, *J. Mol. Biol. 331*, 907−924.
27. Mansy, S. S., Wu, S., and Cowan, J. A. (2004) Iron-sulfur cluster biosynthesis. Biochemical characterization of the conformational dynamics of thermotoga maritima IscU and the relevance for cellular cluster assembly, *279*, 10469−10475.
28. Silberg, J. J., Hoff, K. G., Tapley, T. L., and Vickery, L. E. (2001) The Fe/S assembly protein IscU behaves as a substrate for the molecular chaperone Hsc66 from Escherichia coli, *J. Biol. Chem. 276*, 1696−1700.
29. Laufen, T., Mayer, M. P., Beisel, C., Klostermeier, D., Mogk, A., Reinstein, J., and Bukau, B. (1999) Mechanism of regulation of Hsp70 chaperones by DnaJ cochaperones, *Proc. Natl Acad. Sci. U.S.A. 96*, 5452−5457.
30. Mally, A., and Witt, S. N. (2001) GrpE accelerates peptide binding and release from the high affinity state of DnaK, *Nat. Struct. Biol. 8*, 254−257.
31. Pierpaoli, E. V., Sandmeier, E., Baici, A., Schonfeld, H.-J., Gisler, S., and Christen, P. (1997) The power stroke of the DnaK/DnaJ/GrpE molecular chaperone system, *J. Mol. Biol. 269*, 757−768.

BI0483007